HHS Public Access

Author manuscript

J Heart Lung Transplant. Author manuscript; available in PMC 2024 May 08.

Published in final edited form as:

J Heart Lung Transplant. 2023 September ; 42(9): 1223–1232. doi:10.1016/j.healun.2023.04.002.

Pulsatility and flow patterns across macro- and microcirculatory arteries of continuous-flow left ventricular assist device patients

Eric J. Stöhr, PhD[a,b,#], **Ruiping Ji, PhD**[b], **Giulio Mondellini, MD**[b], **Lorenzo Braghieri, MD**[b,c], **Koichi Akiyama, MD**[d,e,##], **Francesco Castagna, MD**[b,f], **Alberto Pinsino, MD**[b], **John R. Cockcroft, MD**[a,b], **Ronald H. Silverman, MD**[g], **Samuel Trocio**[h], **Oksana Zatvarska, BSc**[b], **Elisa Konofagou, PhD, MSc**[i], **Iason Apostolakis, PhD**[i], **Veli K. Topkara, MD, MSc**[b], **Hiroo Takayama, MD, PhD**[c], **Koji Takeda, MD, PhD**[c], **Yoshifumi Naka, MD, PhD**[c], **Nir Uriel, MD, MSc**[b], **Melana Yuzefpolskaya, MD**[b], **Joshua Z. Willey, MD, MSc**[h], **Barry J. McDonnell, PhD**[a], **Paolo C. Colombo, MD**[b]

[a]School of Sport & Health Sciences, Cardiff Metropolitan University, Cardiff, UK

[b]Department of Medicine, Division of Cardiology, Columbia University Irving Medical Center, New York, New York

[c]Department of Internal Medicine, Cleveland Clinic, Cleveland, Ohio

[d]Department of Medicine, Division of Cardiothoracic Surgery, Columbia University Irving Medical Center, New York, New York

[e]Department of Cardiovascular Surgery, Kyoto Prefectural University of Medicine, Kyoto, Japan

[f]Cardiology Division, Montefiore Medical Center, New York, New York

[g]Department of Ophthalmology, Edward S. Harkness Eye Institute, Columbia University Irving Medical Center, New York, New York

[h]Department of Neurology, Columbia University Irving Medical Center, New York, New York

[i]Department of Biomedical Engineering, Columbia University Irving Medical Center, New York, New York.

Abstract

BACKGROUND: Reduced arterial pulsatility in continuous-flow left ventricular assist devices (CF-LVAD) patients has been implicated in clinical complications. Consequently, recent improvements in clinical outcomes have been attributed to the “artificial pulse” technology inherent to the HeartMate3 (HM3) LVAD. However, the effect of the “artificial pulse” on arterial flow, transmission of pulsatility into the microcirculation and its association with LVAD pump parameters is not known.

Reprint requests: Eric J. Stöhr eric.stoehr@sportwiss.uni-hannover.de.
[#]Now: COR-HELIX (CardiOvascular Regulation and Human Exercise Laboratory – Integration and Xploration), Institute of Sports Science, Leibniz Universität Hannover, 30167 Hannover, Germany
[##]Now: Department of Anesthesiology, Yodogawa Christian Hospital, Osaka, Japan

The authors have no conflicts of interest to disclose.

METHODS: The local flow oscillation (pulsatility index, PI) of common carotid arteries (CCAs), middle cerebral arteries (MCAs) and central retinal arteries (CRAs-representing the microcirculation) were quantified by 2D-aligned, angle-corrected Doppler ultrasound in 148 participants: healthy controls, $n = 32$; heart failure (HF), $n = 43$; HeartMate II (HMII), $n = 32$; HM3, $n = 41$.

RESULTS: In HM3 patients, 2D-Doppler PI in beats with "artificial pulse" and beats with "continuous-flow" was similar to that of HMII patients across the macro- and microcirculation. Additionally, peak systolic velocity did not differ between HM3 and HMII patients. Transmission of PI into the microcirculation was higher in both HM3 (during the beats with "artificial pulse") and in HMII patients compared with HF patients. LVAD pump speed was inversely associated with microvascular PI in HMII and HM3 (HMII, $r^2 = 0.51$, $p < 0.0001$; HM3 "continuous-flow," $r^2 = 0.32$, $p = 0.0009$; HM3 "artificial pulse," $r^2 = 0.23$, $p = 0.007$), while LVAD pump PI was only associated with microcirculatory PI in HMII patients.

CONCLUSIONS: The "artificial pulse" of the HM3 is detectable in the macro- and microcirculation but without creating a significant alteration in PI compared with HMII patients. Increased transmission of pulsatility and the association between pump speed and PI in the microcirculation indicate that the future clinical care of HM3 patients may involve individualized pump settings according to the microcirculatory PI in specific end-organs.

Keywords

HM3; LVAD; pulsatility; microcirculation; HMII

The hallmark of heart failure (HF) is a progressive reduction in cardiac output, resulting in reduced blood flow to the microcirculation of end-organs.[1] Mechanical circulatory support has become an essential therapy to unload the left ventricle (LV) and restore end-organ perfusion in advanced HF.[2] Contemporary continuous-flow left ventricular assist devices (CF-LVADs) are more durable and associated with improved outcomes compared to prior generation pulsatile LVADs. However, they also reduce arterial pulsatility, which, in turn, may compromise the normal in vivo arterial function necessary to provide adequate tissue perfusion.[3–5] Indeed, complications in LVAD patients include a high prevalence of gastrointestinal bleeding (GIB) and cerebral macro–and microbleeds, which may result not only from coagulopathy due to antithrombotic treatment and acquired von Willebrand deficiency,[6] but also, based on imaging and functional studies, from microvascular derangement[7,8] and endothelial dysfunction.[9]

The improved clinical outcomes of the newer generation HeartMate3 device (HM3)[10–14] compared to other CF-LVADs have been attributed to the new technological feature of a regular "artificial pulse," which was primarily designed to improve washout within the pump, resulting in improved hemocompatibility with reduced occurrence of device thrombosis. With the HM3, rates of GIB are also reduced by 17% when compared to prior generation HeartMate II (HMII),[10] however, this complication remains common in HM3 patients at 1 and 2-year follow up.[15–17] Equally, the prevalence of stroke has significantly reduced in HM3 compared with HMII, but hemorrhagic stroke (ischemic stroke with hemorrhagic conversion and primary parenchymal hematomas) remains a clinical

concern.[16–18] Therefore, it is conceivable that the “artificial pulse” acts proximally in the pump to reduce blood stasis but pulsatility may no longer be detectable distally in the microcirculation due to its brief duration (~350ms). Whether transmission of pulsatility into the microcirculation occurs in HM3 patients, and whether LVAD pump speed may further affect distal pulsatility is not known.[19–25]

Although challenging, the accurate measurement of arterial pulsatility in CF-LVAD patients is critical for pathophysiological investigations in this area. In this study we used the spectral analysis of local flow waveforms for quantification of PI in the macro- and microcirculation.[26,27] Importantly, in contrast to pressure-based measurements of pulsatility (e.g., pulse pressure and pulmonary artery pulsatility index), the 2D-Doppler PI represents the oscillation of flow velocities normalized to the mean flow velocity. Notably, novel data show that pressure and flow waveforms do not necessarily correlate.[25] Consequently, to advance our current knowledge on the effects of the “artificial pulse” of HM3 patients, we aimed to: (1) characterize the hemodynamic profile of the elastic central common carotid artery (CCA), medium-sized middle cerebral artery (MCA) and central retinal artery (CRA) (~160 μm in diameter, representing the microcirculation of the eye, as well as, based on the neurology literature, of the brain[28]) in HF patients, HMII patients, HM3 patients (with separate analysis of beats with and without “artificial pulse”) and healthy subjects; (2) determine the transmission of arterial pulsatility from the CCA into the CRA; and (3) determine the association between LVAD pump parameters (speed and PI) and local arterial pulsatility in the microcirculation.

Methods

Study population

Four groups of volunteers were enrolled: (1) HF patients, (2) HF patients implanted with the HMII LVAD, (3) HF patients implanted with HM3 LVAD and (4) healthy volunteers. Healthy individuals were included if they did not have any known/diagnosed chronic diseases including hypertension and diabetes, were not taking any regular medication and did not report a current illness. Heart failure patients were included if they were diagnosed with HF for at least 6 months and had a left ventricular ejection fraction ≤30%. Heart Failure patients were excluded if they were receiving any form of mechanical circulatory support or were clinically unstable. Inpatient and outpatient LVAD patients were included if they were clinically stable, did not require any vasopressors, inotropic support, additional mechanical circulatory support, did not have evidence of carotid stenosis,[29] and were free of acute pain. Some of these patients were also included in a previous publication.[30] The study protocol was approved by the Institutional Review Board of the Columbia University Irving Medical Center.

Local ultrasound assessment of arterial blood flow dynamics

Data collection took place at a single site (Columbia University Irving Medical Center). Local blood flow dynamics were quantified in the CCA, MCA and the CRA. All arteries were assessed using a commercially available ultrasound system (Vivid E90, Milwaukee WI) with the participants in the semi-recumbent position. The order of vascular assessment

was consistent in all participants: central retinal arteries, middle cerebral arteries, and common carotid arteries. For all images, standardization was achieved as per current guidelines, referred to in the respective sections below. Imaging depth was minimized, width and gain were adjusted to enhance the clarity of regions of interest, the color map was adjusted to avoid aliasing and maximize gain, prior to applying pulsed-wave Doppler modalities. For CCA images obtained with the linear array transducer, care was taken that the angle of insonation did not exceed 60 degrees. In all 3 arteries, following identification of a minimum longitudinal portion of each artery, the angle of insonation was aligned in the direction of flow, thus enabling the confident reporting of absolute peak systolic velocity (PSV), minimum diastolic velocity (MDV), and mean flow velocity (MFV) based upon the time-averaged maximum velocity, respectively. PSV, MDV, and MFV were then used to calculate pulsatility index (PI = (PSV-MDV) / MFV) as a parameter used to describe the degree of hemodynamic flow velocity oscillations relative to the mean velocity (obtained from the manufacturer software as the time-averaged mean of the wave contour). A representative example of the CRA assessment is shown in Figure 1. One operator who was blinded to the allocation of patients to the study groups analyzed all the data. All data were analyzed either by automatic edge-detection of the flow velocity signal over 3 to 5 cardiac cycles or, if the quality of tracing was not sufficient according to the operator, by manual tracing of 3 to 5 cardiac cycles. Importantly, with very few exceptions, there was no systematic variability observed. Rather, despite the lack of synchronization between the “artificial pulse” and the native heart beat the blood flow patterns were stable and only rarely deviated (for the purpose of transparency and education, one rare exception is shown in Figure 1, where the third artificial pulse did not have the same effect as the first 2). Data reported in this manuscript represent the average of 3 to 5 cardiac cycles. For HM3 patients only, beats with “artificial pulse” (every 2 seconds) and beats without the “artificial pulse” (i.e., “continuous flow”) were analyzed separately. Heart rate was determined from the ECG tracing inherent to the ultrasound images obtained for flow analysis.

In some patients, data could not be obtained in all 3 arteries. The following reflect the number of participants in whom hemodynamics in the left and right anatomical regions could be obtained, respectively: CCA (Healthy left = 32; Healthy right = 32; HF left = 41; HF right = 34; HMII left = 27; HMII right = 19; HM3 left = 37; HM3 right = 33), MCA (Healthy left = 27; Healthy right = 27; HF left = 37; HF right = 36; HMII left = 25; HMII right = 19; HM3 left = 36; HM3 right = 33;) CRA (Healthy left = 32; Healthy right = 32; HF left = 40; HF right = 34; HMII left = 25; HMII right = 21; HM3 left = 34; HM3 right = 21). Reasons for exclusion were: poor echo window, poor Doppler signal, external wound to the neck due to recent catheterization, presence of a clinically-relevant stenosis (29), eye disease, eye movement that prevented a stable CRA flow signal, and an inability to confidently locate the MCA.

Following a comparison of left- vs right-sided pulsatility, which revealed no systematic difference between the 2 sides (Two-way ANOVA of PI in the left vs right CCA, MCA, and CRA, between HMII and HM3 patients: $p = 0.75$, $p = 0.84$, and $p = 0.21$, respectively), data in this manuscript represent the average of both left and right-sided measurements. In those patients in whom measurements were not obtained successfully on both sides, data from only 1 side were included because of the aforementioned lack of systematic differences

between the 2 sides. Consequently, the final analyses included slightly different sample sizes among arteries. Specifically, CCA (Healthy = 32; HF = 41; HMII = 28; HM3 = 39), MCA (Healthy = 31; HF = 39; HMII = 28; HM3 = 38), CRA (Healthy = 32; HF = 42; HMII = 25; HM3 = 33).

Common carotid arteries—CCA image acquisition was standardized by ensuring that the anterior and posterior walls were clearly defined and, ideally, the intima-media boundary was visible in both. Doppler sampling was performed 2 to 3 cm proximal to the carotid bifurcation (internal / external carotid arteries). The resultant flow velocity signal was recorded for offline analysis.

Middle cerebral arteries—For the assessment of MCA hemodynamics, the artery was identified from an initial ultrasonic window close to the participant's temple, and then optimized by angulation of the transducer and optimization of the color Doppler map. The transducer angle was adjusted until a clear longitudinal section of the middle cerebral artery around 50 mm depth was visualized consistently across a few cardiac cycles. Then, a pulsed wave Doppler sample was positioned in the middle of the visible section, avoiding sampling close to any possible bifurcations. The resultant flow velocity signal was recorded for offline analysis. We would like to highlight the importance of this approach in relation to a confident assessment of the MCA velocities in LVAD patients. Without the 2D location and optimization of the MCA, it would be near impossible to determine the correct cerebral artery due to the similarities in the Doppler signal between different arteries (in contrast to healthy humans, where the blind assessment is supported by the distinctive shapes of the different cerebral arteries), thus representing an important methodological step in the confident quantification of cerebral hemodynamics in LVAD patients.

Central retinal arteries—The ultrasound transducer was placed centrally over the closed eyelid, and tilted cranially or caudally until the optic nerve was clearly visible and in the center of the ultrasound sector. Employing a horizontal scan plane and with the aid of the color Doppler map and further minor adjustment of the probe angle, a longitudinal view of the central retinal artery was obtained. A pulsed-wave Doppler sample volume was placed a few millimeters posterior to the optic nerve head. The resultant flow velocity signal was recorded for offline analysis.

Transmission of arterial hemodynamics

Transmission of flow pulsatility in to the microcirculation was determined by dividing the PI of the CRA by the PI of the CCA.[31] The average transmission of the left and the right side was used for statistical analysis.

Statistical analyses

Statistical outcomes with $p < 0.05$ were considered significant. For the main comparisons, including HM3 sub-group analyses, differences between groups were first determined with one-way analysis of variance (ANOVA) with Tukey's Multiple Comparisons post hoc test. However, Bartlett's test for equal variances revealed unequal variances in many data sets, including pulsatility in the CCA, MCA, and CRA. Therefore, the Kruskal-Wallis test was

consistently used with Dunn's Multiple Comparison test as a post hoc evaluation of the study groups with both HM3 data obtained during beats with "continuous flow" and beats with "artificial pulse." Relationships between LVAD pump parameters (speed and PI) and 2D-Doppler PI were determined using linear regression analysis. All data were analyzed using GraphPad Prism for Windows (Version 5.01, GraphPad Software, Inc., San Diego, CA).

Results

Baseline characteristics

Our final cohort included a total of 148 participants: HF: $n = 43$; HMII: $n = 32$; HM3: $n = 41$; healthy controls: $n = 32$. Baseline demographics and clinical characteristics are shown in Table 1. INTERMACS profile at the time of LVAD implant did not differ between HMII and HM3 patients. Healthy subjects were younger and had a lower BMI. Pump power, flow, and pulsatility index were higher in HMII than HM3. Due to the consecutive recruitment, duration of LVAD support was longer in HMII compared with HM3 patients. LVAD patients were more likely to receive warfarin compared to HF patients. Some differences in medication between the patient groups reflect standard practices in the treatment of HF and LVAD patients (Table 1).

Hemodynamic profiles in the macro- and microcirculation

Hemodynamic results are shown in Table 2 and Figure 3. In all 3 arteries, PSV was markedly lower in HMII and HM3 groups compared with HF patients and healthy controls; MFV was similar in HF, HMII and HM3, and was significantly lower in these 3 groups compared to healthy controls in the CCA and MCA and, numerically, in the CRA. In all 3 arteries, the MDV was lower in HF compared with HMII and HM3 "continuous-flow," reflecting the continuous flow in LVAD patients which prevents the normal diastolic drop in flow.

In all 3 arteries, the 2D-Doppler PI was markedly lower in HMII and HM3 groups compared with HF patients and healthy controls. Notably, the PI of HM3 "artificial pulse" was significantly higher than HM3 "continuous-flow," and numerically higher than HMII although this latter difference was not statistically significant (Figure 3). This difference in 2D-Doppler PI was explained entirely by the sudden drop in flow velocity in the beats with an "artificial pulse," which was reflected by the significantly lower MDV in this group. In other words, our data reveal that the increased PI of HM3 "artificial pulse" is caused by a reduced diastolic flow, not by an increased systolic flow. A schematic of the hemodynamic profiles of the CRA is shown in Figure 2.

Transmission of pulsatility from the macro- into the microcirculation

Transmission of pulsatility from the CCA into the CRA was greater in HMII and in HM3 "artificial pulse" compared with HF, as evidenced by a higher PI ratio between the CCA and the CRA (Figure 4).

Relationships between LVAD pump parameters and 2D-Doppler PI in the microcirculation

LVAD pump speed was significantly inversely associated with 2D-Doppler PI in the CRA. This association was stronger in HMII compared with HM3. In contrast, LVAD pump PI was only associated with microcirculatory PI in HMII patients, while no relationship was found in HM3, neither during the “continuous-flow” phase nor in beats with “artificial pulse” (Figure 5).

Discussion

Our study provides several novel findings. First, the artificial pulsatility of the HM3 is clearly detectable in the central and medium-sized arteries as well as in the microcirculation. Second, in HM3 patients, the 2D-Doppler PI was higher in beats with “artificial pulse” than in beats with “continuous flow” throughout these vascular compartments; however, although nominally higher, the “artificial pulse” PI of the HM3 was not statistically different from the PI of the HMII. Third, transmission of pulsatility into the microcirculation of HMII and HM3 was greater compared with HF patients. Fourth, in both HMII and HM3 patients, LVAD pump speed was inversely associated with the 2D-Doppler PI although less so for HM3 than the HM2, particularly in beats with “artificial pulse,” while LVAD pump PI was only associated with the 2D-Doppler PI in HMII patients. Together, the data indicate a consistent pattern of hemodynamics from macro- to microcirculation.

Besides the magnetic levitation, the main technological change of the HM3 pump compared with its predecessors is the introduction of the “artificial pulse,” which was designed to reduce the occurrence of pump thrombosis and associated complications. While the clinical data indeed support a successful reduction in hemocompatibility-related adverse events,[10,14,16,17] HM3 patients still experience frequent vascular complications.[15] One reason could be that the interaction between the mechanical device and the arterial biology of the patient is still not favorable. Ongoing debates about the role of pulsatility have raised the hope that a positive effect of the HM3 “artificial pulse” could be an increased *arterial* pulsatility (i.e., not just reducing thrombogenicity *inside* the pump but also vascular derangement *outside* it), resulting in an improved end-organ perfusion and reduction of the above complications. Indeed, loss of pulsatility has been associated with several pathobiological processes in the vasculature including reduction in nitric oxide production, and increase in arterial stiffness.[3,32,33] Increased smooth muscle content has been also reported, in particular for the aorta.[33,34] Increased central arterial (aortic or carotid) stiffness would be expected to reduce the attenuation of pulsatility and, hence, transmit more pulsatility downstream. Equally, increased arterial tone in the peripheral vasculature could increase the local (downstream) pulsatility by augmenting any pulsatility that has been received from upstream arteries. Theoretically, prior to the present study, it was possible that the “artificial pulse” of the HM3 would not transmit into the peripheral circulation, since each phase of the HM3 pump speed modulation is short-lived (−2,000 rpm from baseline lasting for 150 msec, followed by +2,000 rpm from baseline lasting for 200 msec). Here, we report, for the first time, that the “artificial pulse” of the HM3 is clearly detectable across several arterial compartments including the microcirculation. While this was observed in selected arterial beds, the remarkably consistent pattern suggests

that it might be present across the whole body although this requires further experimental confirmation. Moreover, the effect of the “artificial pulse” on the arterial biology of HM3 patients does not reflect an increased pulsatility in the typical sense. Instead, the pulsatility of the “artificial pulse” results in an immediate, and marked reduction in blood flow velocity in all 3 arteries, which is the opposite effect of increased pulsatility in other populations, for example hypertensive patients. This observation is supported by the reduction in MDV during the beats with “artificial pulse.” Intriguingly, the subsequent increase in LVAD pump speed during the “artificial pulse” did not have the opposite effect since PSVs were similar across the “continuous flow” and “artificial pulse” phases. The biological effect of this “reverse pulse” on vascular cell mechanotransduction remains to be determined but it is possible that the normal vascular mechanotransduction is markedly altered.[3] In particular the altered shear stress is expected to have a significant impact on the typical mechanical and signaling processes. Whether the temporary but marked blood volume withdrawal caused by the artificial pulse can be likened to a suction effect and cause similar mechanotransduction to normal pulsatility requires further study. Notably, and irrespective of the upward or downward inflection of the pulse profile,[35] we observed a significant overlap in the PI between HMII and HM3, which was only nominally higher in the HM3 “artificial pulse.” Whether this marginal increase in pulsatility with a reverse profile is sufficient to improve endothelial function and vascular tone/regulation in HM3 patients warrants further investigation. Recent data of an increased vasoreactivity of HM3 patients compared with HMII are supportive of this hypothesis,[30] but further data are needed to determine the impact of baseline PI vs a reactive response (e.g., to a metabolic challenge, a hypertensive surge or a hypotensive dip). Moreover, there may be a U-shaped relationship between pulsatility and adverse events, since pulsatility in LVAD occurs in addition to continuous flow–a situation that is unique since the normal alteration between systolic and diastolic phases is caused by an intermittent supply of blood to the circulation. Therefore, the margin of the optimal pulsatility, situated between not enough and too much pulsatility, may be smaller than in the general population. Interestingly, with respect to the hemodynamics underpinning mucosal bleeding due to AGD formation, Patel et al[36,37] have elegantly shown that mucosal AGDs are already prevalent in HF patients, although the severity was double on CF LVAD support. Our study indicates that MFV is reduced in HF patients compared with healthy subjects while Doppler PI is similar. These results suggest that a reduction in average flow (perfusion) may be implicated in AGD formation in HF patients (“first hit”). After CF-LVAD implantation, the additional reduction in arterial pulsatility and energy flow content may further impair tissue perfusion and exacerbate this phenomenon (“second hit”). Notably, recent experimental data on synchronization of the “artificial pulse” with the cardiac cycle did show a large effect on pulsatility for some settings.[24] Whether this strategy may translate into improved pulsatility within the microcirculation and result in better outcomes remains to be established.

Our data further indicates a greater transmission of pulsatility from the CCA to the CRA in HMII and HM3 than in HF patients. Considering previous reports of an increased arterial stiffness in HMII patients[34,38,39] and the potential for a diverse response depending on the hemodynamics prior to LVAD implantation,[39] our data suggest that vascular stiffness may be similarly increased in HM3 patients. Therefore, we also think that caution is warranted

when aiming to increase pulsatility in LVAD patients by, for example, synchronizing the artificial pulse with the native heart contraction,[24] since this may lead to an excessive PI in the microcirculation. This may be exacerbated by a possible dysfunction of the arterial vasomotor tone in both HMII and HM3 patients. Since HM3 patients do not have a greater PSV, these hemodynamics likely translate into reduced stimulation of carotid baroreceptors with ensuing increases in vascular tone similar to that seen in HMII patients.[20] Whether, and to which extend, structural and/or functional vascular impairment explains the proportionately greater transmission of pulsatility into the microcirculation of HMII and HM3 patients deserves targeted investigation in the future. We note that we measured transmission into the microcirculation in the retina, a region that has substantial overlaps with vascular biology in the brain. Altered hemodynamics in the microcirculation of the brain have been increasingly linked to cerebral small vessel disease, such as white matter hyper-intensities, and with cognitive impairment in part due to reduced clearance of amyloid via the brain lymphatics.[7,40–42]

From invasive and noninvasive blood pressure recordings in the macrocirculation, it has long been known that a higher pump speed reduces pulsatility in CF-LVAD patients since greater unloading of the LV results in lower pulsatile output from the native heart, and, simultaneously, more CF from the LVAD into the aorta. Consequently, we expected a stronger association between LVAD pump speed and pulsatility closer to the LVAD outflow graft, that is, in the CCA. Instead, relationships were comparatively low (or nonexistent) in the CCA, possibly because of the structural properties of the CCA caused by the individual HF history. This fits with the observation of a large variation of aortic stiffness prior to LVAD implantation,[39] suggesting that the HF history may be a major determinant of the impact of pump speed on central arterial pulsatility. Therefore, our results indicate, for the first time, that the peripheral microcirculation may be more dependent on LVAD speed than the central arteries. We speculate that this may be related to altered hemodynamics in the largest sense, including pulse wave transmission, impedance, wave reflection as well as arterial compliance in LVAD patients.[25,43] However, it is worth noting that LVAD pump speed explained still only 20% to 50% of the variance of microcirculatory PI in HMII and HM3 patients. Thus, it is important to not rely on pump speed alone as an indicator of microcirculatory pulsatility. Whether assessments of microcirculatory PI should be performed in conjunction with or independent of LVAD speed optimization when confirming LVAD settings for patient care remains to be studied, in particular in HM3 patients, who had less of an association between LVAD pump speed and 2D-Doppler PI.

The observed discrepancy in the association between pump PI and 2D-Doppler PI in HMII and HM3 patients was somewhat surprising. A possible explanation is the known difference between HMII and HM3 power-flow characteristics, affecting their respective calculations of pump PI. Specifically, the estimation of HMII PI can be confounded in situations of low flows and simultaneously high pump speeds (e.g., aggravated during hypertension); conversely, the calculations of HM3 PI can be confounded at high flows and simultaneously low speeds (e.g., aggravated during hypotension). Thus, it is tempting to attribute the above discrepancy to this intrinsic difference between HMII and HM3 PI calculation. Formal hemodynamic “ramp” studies with serial pump speed adjustments in the individual

patient appear warranted to better clarify the association between pump parameters and microvascular PI.

Some limitations should be acknowledged. The studied cohort was relatively small, including predominantly male participants, thus limiting generalizability. Our study groups had important baseline differences in demographics and medication use that could have affected the observations. No blood pressure measurements were taken, since no reliable and valid method exists for the noninvasive assessment of blood pressure in the primary patient population of this study that is, the HM3. Furthermore, we are unable to report precisely on the patient fluid status or cardiac filling pressures, 2 aspects that deserve focused attention in the future. Our assessment of the microvasculature was limited to the CRA, thus we can only extrapolate that our observations apply to different vascular beds. Although we did not observe any consistent pattern in those patients in whom part of the data could not be obtained, it is possible that this may have been related to altered local hemodynamics. Inclusion of stable LVAD patients may have added a selection bias and future studies may wish to include patients with acute complications to determine whether microcirculatory hemodynamics may differ.

In summary, these data indicate that the forces generated by the LVAD, whether continuous or intermittent, impact the hemodynamics of the microcirculation. They also indicate that transmission of pulsatility is increased in CF-LVAD patients possibly reflecting increased arterial stiffness and/or vascular tone, and that LVAD pump speed modulates the microcirculatory PI in HMII and HM3 patients. Together, these flow profile analyses offer important insight into the interaction between forces generated by the implanted LVAD technology and local arterial structure and function. Thus, the findings have important implications on the ongoing clinical outcomes noted with microvascular dysfunction in this population. Future investigations may determine whether changes in width and duration of the “artificial pulse” can further impact arterial hemodynamics and possibly contribute to an improved patient outcome.

Disclosure statement

This project has received funding from the European Union’s Horizon 2020 research and innovation program under the Marie Skłodowska-Curie grant agreement No 705219. This study was also supported by the Lisa and Mark Schwartz Program to Reverse Heart Failure at New York – Presbyterian Hospital/ Columbia University, NIH grant P30 EY019007 and an unrestricted grant to the Department of Ophthalmology of Columbia University from Research to Prevent Blindness.

References

1. Dhakal BP, Malhotra R, Murphy RM, et al. Mechanisms of exercise intolerance in heart failure with preserved ejection fraction: the role of abnormal peripheral oxygen extraction. Circ Heart Fail 2015;8:286–94. [PubMed: 25344549]
2. Uriel N, Sayer G, Annamalai S, Kapur NK, Burkhoff D. Mechanical unloading in heart failure. J Am Coll Cardiol 2018;72:569–80. [PubMed: 30056830]
3. Hahn C, Schwartz MA. Mechanotransduction in vascular physiology and atherogenesis. Nat Rev Mol Cell Biol 2009;10:53–62. [PubMed: 19197332]
4. Inamori S, Shirai M, Yahagi N, et al. A comparative study of cerebral microcirculation during pulsatile and nonpulsatile selective cerebral perfusion: assessment by synchrotron radiation microangiography. ASAIO J 2013;59:374–9. [PubMed: 23820275]

5. Cornwell WK 3rd, Tarumi T, Aengevaeren VL, et al. Effect of pulsatile and nonpulsatile flow on cerebral perfusion in patients with left ventricular assist devices. J Heart Lung Transplant 2014;33:1295–303. [PubMed: 25307621]
6. Sakatsume K, Saito K, Akiyama M, et al. Association between the severity of acquired von Willebrand syndrome and gastrointestinal bleeding after continuous-flow left ventricular assist device implantation. Eur J Cardiothorac Surg 2018;54:841–6. [PubMed: 29741685]
7. Murase S, Okazaki S, Yoshioka D, et al. Abnormalities of brain imaging in patients after left ventricular assist device support following explantation. J Heart Lung Transplant 2020;39:220–7. [PubMed: 31843457]
8. Yoshioka D, Okazaki S, Toda K, et al. Prevalence of cerebral microbleeds in patients with continuous-flow left ventricular assist devices. J Am Heart Assoc 2017;6:10.
9. Witman MA, Garten RS, Gifford JR, et al. Further peripheral vascular dysfunction in heart failure patients with a continuous-flow left ventricular assist device: the role of pulsatility. JACC Heart Fail 2015;3:703–11. [PubMed: 26277768]
10. Mehra MR, Uriel N, Naka Y, et al. A fully magnetically levitated left ventricular assist device - final report. N Engl J Med 2019;380:1618–27. [PubMed: 30883052]
11. Mehra MR, Naka Y, Uriel N, et al. A fully magnetically levitated circulatory pump for advanced heart failure. N Engl J Med 2017;376:440–50. [PubMed: 27959709]
12. Mehra MR, Goldstein DJ, Uriel N, et al. Two-year outcomes with a magnetically levitated cardiac pump in heart failure. N Engl J Med 2018;378:1386–95. [PubMed: 29526139]
13. Colombo PC, Mehra MR, Goldstein DJ, et al. Comprehensive analysis of stroke in the long term cohort of the MOMENTUM 3 study: a randomized controlled trial of the HeartMate 3 versus the HeartMate II cardiac pump. Circulation 2018. In press.
14. Uriel N, Colombo PC, Cleveland JC, et al. Hemocompatibility-related outcomes in the MOMENTUM 3 trial at 6 months: a randomized controlled study of a fully magnetically levitated pump in advanced heart failure. Circulation 2017;135:2003–12. [PubMed: 28385948]
15. Mehra MR, Goldstein DJ, Uriel N, et al. Two-year outcomes with a magnetically levitated cardiac pump in heart failure. N Engl J Med 2018;378:1386–95. [PubMed: 29526139]
16. Hanke JS, Dogan G, Zoch A, et al. One-year outcomes with the HeartMate 3 left ventricular assist device. J Thorac Cardiovasc Surg 2018;156:662–9. [PubMed: 29525258]
17. Zimpfer D, Gustafsson F, Potapov E, et al. Two-year outcome after implantation of a full magnetically levitated left ventricular assist device: results from the ELEVATE Registry. Eur Heart J 2020;41:3801–9. [PubMed: 33107561]
18. Colombo PC, Mehra MR, Goldstein DJ, et al. Comprehensive analysis of stroke in the long-term cohort of the MOMENTUM 3 study. Circulation 2019;139:155–68. [PubMed: 30586698]
19. Cornwell W, Tarumi T, Lawley J, Ambardekar AV. CrossTalk opposing view: blood flow pulsatility in left ventricular assist device patients is NOT essential to maintain normal brain physiology. J Physiol 2018;597:357–9. [PubMed: 30560586]
20. Cornwell WK 3rd, Tarumi T, Stickford A, et al. Restoration of pulsatile flow reduces sympathetic nerve activity among individuals with continuous-flow left ventricular assist devices. Circulation 2015;132:2316–22. [PubMed: 26510698]
21. St€ohr EJ, McDonnell BJ, Colombo PC, Willey JZ. CrossTalk proposal: blood flow pulsatility in left ventricular assist device patients is essential to maintain normal brain physiology. J Physiol 2018. In press.
22. St€ohr EJ. Bionic women and men. Stonehouse, United Kingdom: ResearchFeatures; 2018 In Press.
23. Castagna F, Stohr EJ, Pinsino A, et al. The unique blood pressures and pulsatility of LVAD patients: current challenges and future opportunities. Curr Hypertens Rep 2017;19:85. [PubMed: 29043581]
24. May-Newman K A mathematical model of artificial pulse synchronization for the HeartMate3 left ventricular assist device. ASAIO J 2022;69:284–9. [PubMed: 35797437]
25. Adji A, Shehab S, Jain P, Robson D, Jansz P, Hayward CS. Arterial compliance and continuous-flow left ventricular assist device pump function. ASAIO J 2022;68:925–31. [PubMed: 35544445]

26. Gosling RG, King DH. Arterial assessment by Doppler-shift ultrasound. Proc R Soc Med 1974;67:447–9. [PubMed: 4850636]
27. Chuang SY, Cheng HM, Bai CH, Yeh WT, Chen JR, Pan WH. Blood pressure, carotid flow pulsatility, and the risk of stroke: a community-based study. Stroke 2016;47:2262–8. [PubMed: 27491737]
28. van Dinther M, Voorter PHM, Schram MT, et al. Retinal microvascular function is associated with the cerebral microcirculation as determined by intravoxel incoherent motion MRI. J Neurol Sci 2022;440:120359. [PubMed: 35917773]
29. Kiyatkin ME, Zuver AM, Gaudig A, et al. Carotid artery structure and hemodynamics and their association with adverse vascular events in left ventricular assist device patients. J Artif Organs 2021;24:182–90. [PubMed: 33459911]
30. Stöhr EJ, Ji R, Akiyama K, et al. Cerebral vasoreactivity in HeartMate 3 patients. J Heart Lung Transplant 2021;40:786–93. [PubMed: 34134913]
31. Beach KW, Bergelin RO, Leotta DF, et al. Standardized ultrasound evaluation of carotid stenosis for clinical trials: University of Washington Ultrasound Reading Center. Cardiovasc Ultrasound 2010;8:39. [PubMed: 20822530]
32. Nakano T, Tominaga R, Nagano I, Okabe H, Yasui H. Pulsatile flow enhances endothelium-derived nitric oxide release in the peripheral vasculature. Am J Physiol Heart Circ Physiol 2000;278:H1098–104. [PubMed: 10749703]
33. Ambardekar AV, Stratton MS, Dobrinskikh E, et al. Matrix-degrading enzyme expression and aortic fibrosis during continuous-flow left ventricular mechanical support. J Am Coll Cardiol 2021;78:1782–95. [PubMed: 34711337]
34. Ambardekar AV, Hunter KS, Babu AN, Tuder RM, Dodson RB, Lindenfeld J. Changes in aortic wall structure, composition, and stiffness with continuous-flow left ventricular assist devices: a pilot study. Circ Heart Fail 2015;8:944–52. [PubMed: 26136459]
35. Pagani FD. Continuous-flow rotary left ventricular assist devices with “3rd generation” design. Semin Thorac Cardiovasc Surg 2008;20:255–63. [PubMed: 19038736]
36. Patel SR, Madan S, Saeed O, et al. Association of nasal mucosal vascular alterations, gastrointestinal arteriovenous malformations, and bleeding in patients with continuous-flow left ventricular assist devices. JACC Heart Fail 2016;4:962–70. [PubMed: 27744088]
37. Patel SR, Vukelic S, Chinnadurai T, et al. Gastrointestinal angiodysplasia in heart failure and during CF LVAD support. J Heart Lung Transplant 2022;41:129–32. [PubMed: 34911655]
38. Patel AC, Dodson RB, Cornwell WK 3rd, et al. Dynamic changes in aortic vascular stiffness in patients bridged to transplant with continuous-flow left ventricular assist devices. JACC Heart Fail 2017;5:449–59. [PubMed: 28285118]
39. Rosenblum H, Pinsino A, Zuver A, et al. Increased aortic stiffness is associated with higher rates of stroke, gastrointestinal bleeding and pump thrombosis in patients with a continuous flow left ventricular assist device. J Card Fail 2021;27:696–9. [PubMed: 33639317]
40. Michelis KC, Zhong L, Tang WHW, et al. Durable mechanical circulatory support in patients with amyloid cardiomyopathy: insights from INTERMACS. Circ Heart Fail 2020;13:e007931. [PubMed: 33164568]
41. DeSimone CV, Graff-Radford J, El-Harasis MA, Rabinstein AA, Asirvatham SJ, Holmes DR Jr. Cerebral amyloid angiopathy: diagnosis, clinical implications, and management strategies in atrial fibrillation. J Am Coll Cardiol 2017;70:1173–82. [PubMed: 28838368]
42. Fan TH, Cho SM, Prayson RA, Hassett CE, Starling RC, Uchino K. Cerebral microvascular injury in patients with left ventricular assist device: a neuropathological study. Transl Stroke Res 2022;13:257–64. [PubMed: 34494179]
43. Vlachopoulos C, O’Rourke M, and Nichols WW (2011). McDonald’s Blood Flow in Arteries: Theoretical, Experimental and Clinical Principles (6th ed.). CRC Press.

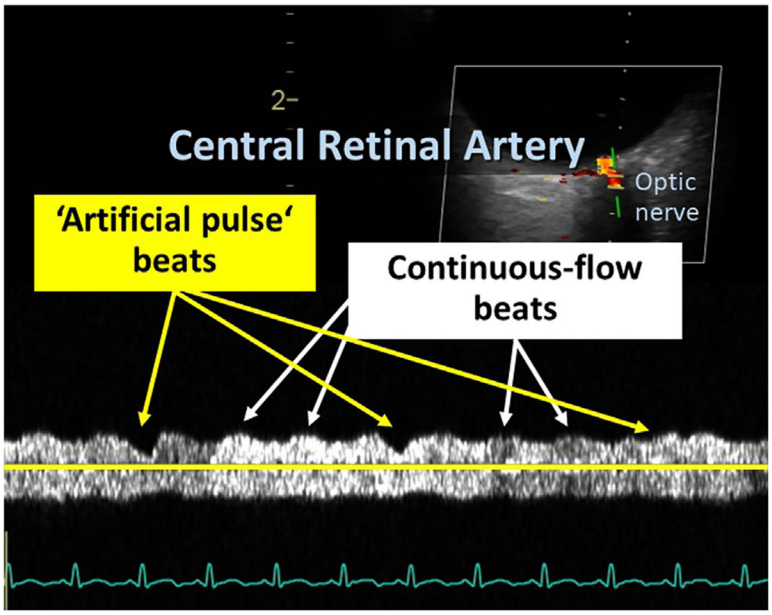

Figure 1.

Ultrasound 2D-Doppler signal in the central retinal artery (microcirculation) of a representative HM3 patient. The occurrence of the "artificial pulse" every 2 sec is asynchronous to the native cardiac cycle. The reduction in pump speed (−2,000 rpm) at the onset of the "artificial pulse" generates a clear downward incision in the ultrasound signal, while there is no increase in flow velocity during the subsequent phase of increased pump speed (+4,000 rpm). Occasionally, as is the case in the third "artificial pulse," the effect of the initial deceleration is less discernible.

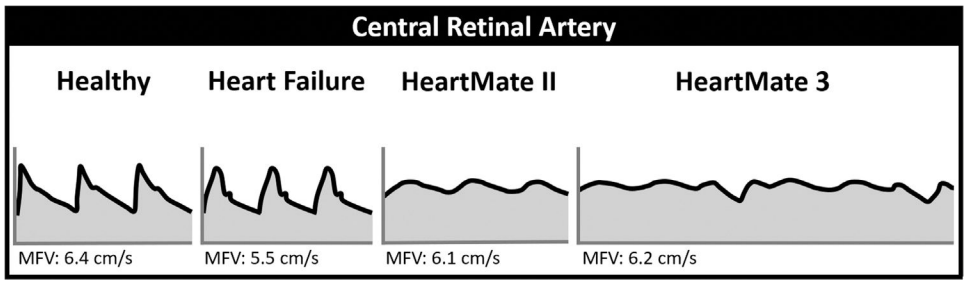

Figure 2.

Schematic representation of microcirculatory hemodynamics in the four study groups. The waveforms represent the mean patterns of each study group as investigated in the central retinal artery (=microcirculation). Mean flow velocity (MFV) is shown numerically, emphasizing that marked differences in blood flow *patterns* can exist in the presence of a similar mean flow velocity. *Note: to extend the insight into this study's results, MFV data here are reported as the numerical mean, as opposed to the median reported elsewhere in the manuscript.*

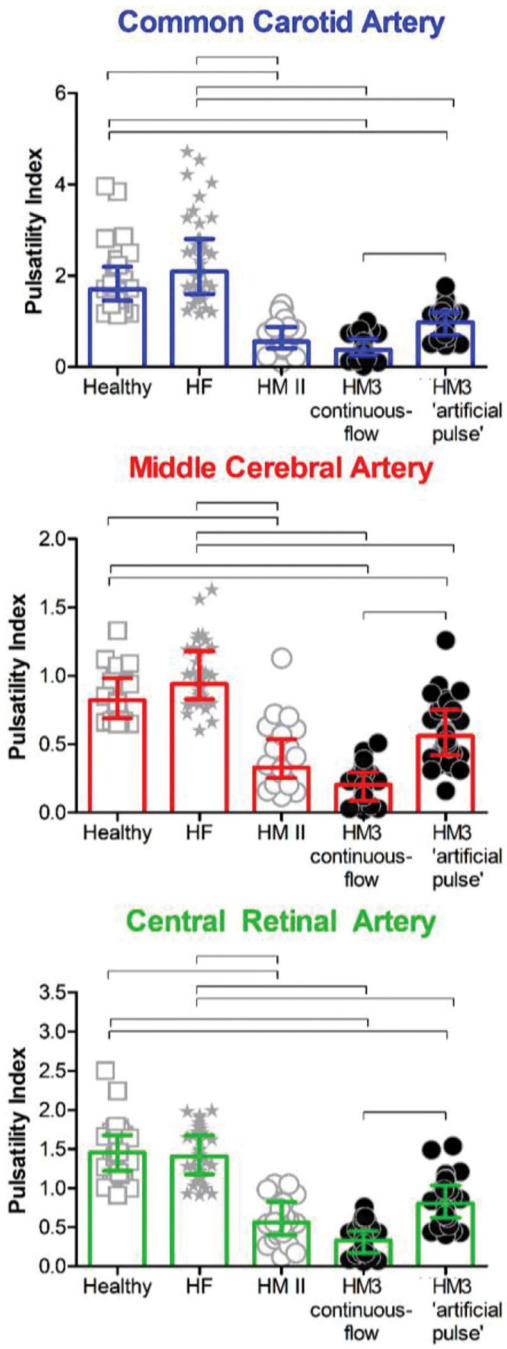

Figure 3.

Arterial hemodynamics of the Common Carotid Artery (CCA), Middle Cerebral Artery (MCA) and Central Retinal Artery (CRA). Moving from large and middle size arteries into the microcirculation, the pulsatility index (PI) was consistently lower in both HMII and HM3 patients, without significant differences between the 2 LVAD groups. Data are shown as median and interquartile range. Lines indicate a *p-value* of < 0.05 between 2 groups.

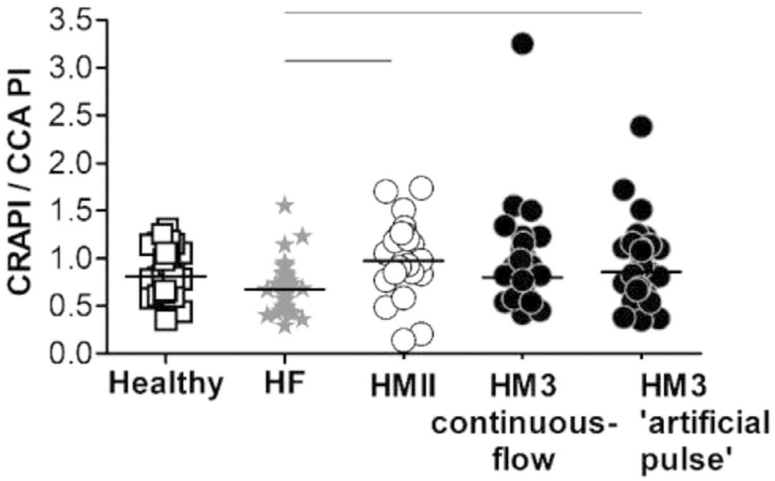

Figure 4.

Transmission of pulsatility into the microcirculation. Both HMII patients and HM3 patients (during the “artificial pulse” phase) had a greater transmission of PI into the microcirculation as evidenced by a higher CCA/CRA PI ratio compared with HF patients.

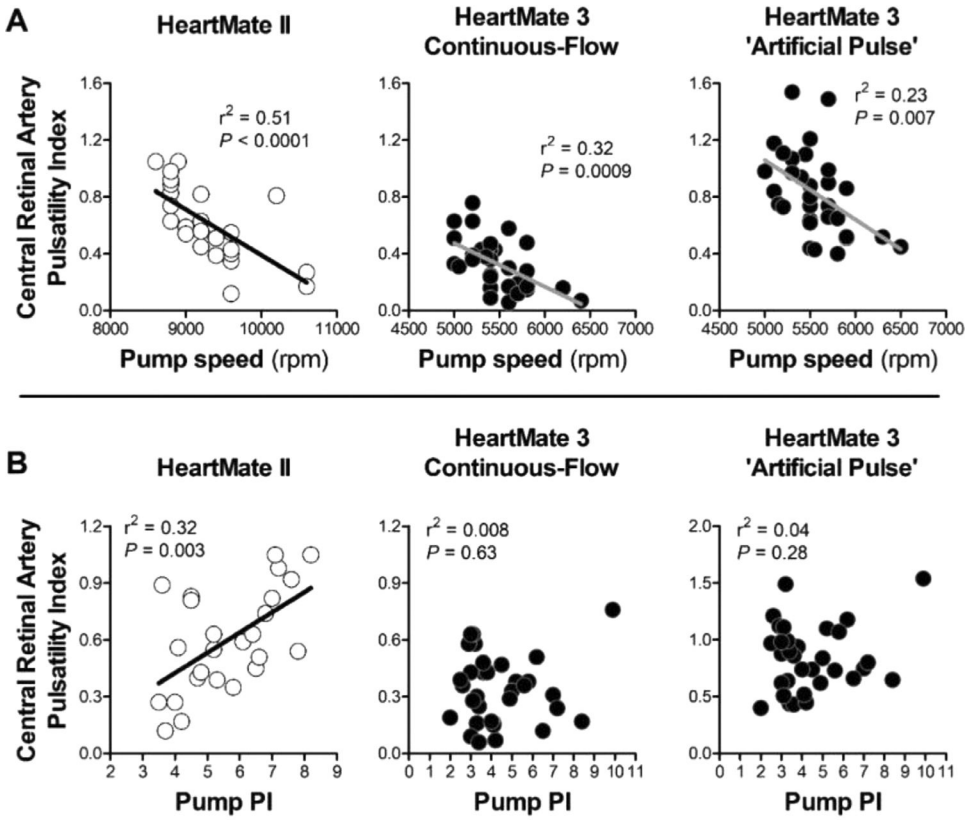

Figure 5.

Relationships between LVAD pump parameters and 2D-Doppler PI in the microcirculation. LVAD pump speed was associated with the 2D-Doppler PI of the CRA in both HMII and HM3 patients; LVAD pump PI was only associated with the 2D-Doppler PI in HMII patients.

Table 1

Clinical Characteristics

	Healthy controls	Heart Failure	HM II	HM3	P-value
Age, y	46 [34–56]	61 [53–68] *	60 [44–76] *	61 [49–71] *	$p < 0.0001$
Female sex, n (%)	11 (34)	9 (21)	6 (19)	5 (12)	$p = 0.14$
BMI, kg/m^2	24.2 [21.7–25.6]	30.2 [24.9–34.5] *	30.0 [23.2–34.3] *	26.2 [23.2–28.8] $	$p < 0.0001$
Race or ethnic group, n (%)					
Black	3 (9)	8 (19)	9 (28)	8 (20)	$p < 0.0001$
White	5 (16)	26 (60)	19 (59)	29 (71)	
Asian	19 (59)	3 (7)	2 (6)	3 (7)	
Other	5 (16)	6 (14)	2 (6)	1 (2)	
Destination therapy, n (%)			28 (88)	29 (71)	$p = 0.09$
Ischemic pathogenesis, n (%)		23 (53)	15 (47)	23 (56)	$p = 0.73$
LVEF, %		15 [13–23]	13 [13–18]	18 [13–21]	$p = 0.21$
LVAD power (W)			5.6 [4.6–6.2]	3.8 [3.6–4.2]	$p < 0.0001$
LVAD speed (rpm)			9200 [8825–9600]	5400 [5200–5600]	
LVAD flow (L/min)			5.4 [4.3–5.9]	4.2 [3.7–5.0]	$p < 0.0001$
LVAD Pulsatility Index			5.5 [4.5–7.0]	4.1 [3.3–5.7]	$p = 0.002$
Duration of LVAD suppport (days)			1269 [816–2000]	29 [17–242]	$p < 0.0001$
INTERMACS profile, n (%)					
1–3			27 (84)	36 (88)	$p = 0.47$
4–5			2 (6)	5 (12)	
NYHA class, n (%)					
1 and 2		6 (14)			
3 & 4	0 (0)	36 (86)			
Medical history, n (%)					
Atrial fibrillation		19 (44)	14 (44)	13 (32)	$p = 0.43$
Diabetes mellitus		15 (35)	12 (38)	16 (39)	$p = 0.92$
Stroke		6 (14)	4 (13)	10 (24)	$p = 0.29$
Hypertension		33 (77)	21 (66)	28 (68)	$p = 0.53$
Carotid artery disease		6 (14)	11 (34)	11 (27)	$p = 0.11$

	Healthy controls	Heart Failure	HM II	HM3	P-value
Peripheral artery disease		1 (2)	5 (16)	9 (22)	$p = 0.02$
Medication, n (%)					
Warfarin		6 (14)	22 (69)	34 (83)	$p < 0.0001$
Statin		26 (60)	12 (38)	20 (49)	$p = 0.14$
ARB		12 (28)	6 (19)	7 (17)	$p = 0.44$
ASA		27 (63)	32 (76)	35 (90)	$p = 0.02$
Dypiridamlole		0 (0)	9 (21)	1 (3)	$p < 0.0001$
Calcium channel blockers		1 (2)	4 (10)	8 (21)	$p = 0.03$
Thiazide diuretics		1 (2)	0 (0)	3 (8)	$p = 0.18$
Hydralazine		4 (9)	2 (5)	0 (0)	$p = 0.16$
Amiodarone		17 (40)	13 (31)	16 (41)	$p = 0.99$
Sildenafil/Tadalafil		1 (2)	5 (12)	11 (28)	$p = 0.005$
Beta-blocker		37 (86)	27 (84)	27 (66)	$p = 0.05$
ACE-inhibitor		4 (9)	7 (22)	3 (7)	$p = 0.13$

*
and
$
is p < 0.05.

Table 2

Hemodynamic Parameters

	Healthy controls	Heart failure	HM II	HM3 continuous-flow	HM3 'artificial pulse'	p-value
Common Carotid Artery (CCA)	(*n* = 32)	(*n* = 41)	(*n* = 28)	(*n* = 39)	(*n* = 39)	
Peak systolic flow velocity, PSV (cm/s)	77 [55–77]	67 [32–46]	42 [32–46][a,b]	40 [32–49][a,b]	43 [35–55][a,b]	$p < 0.0001$
Minimum diastolic flow velocity, MDV (cm/s)	20 [18–21]	14 [7–17][a]	21 [17–26][b]	28 [21–33][a,b]	15 [11–21][c,d]	$p < 0.0001$
Mean flow velocity, MFV (cm/s)	36 [33–38]	28 [24–33][a]	30 [23–34][a]	33 [26–40]	30 [24–39][a]	$p < 0.0001$
Pulsatility Index, PI	1.70 [1.45–2.20]	2.09 [1.60–2.81]	0.55 [0.40–0.88][a,b]	0.37 [0.25–0.61][a,b]	0.97 [0.70-1.19][a,b,d]	$p < 0.0001$
MIDDLE CEREBRAL ARTERY (MCA)	(*n* = 31)	(*n* = 39)	(*n* = 28)	(*n* = 38)	(*n* = 38)	
Peak systolic flow velocity, PSV (cm/s)	88 [73–99]	76 [42–67]	55 [42–67][a,b]	52 [41–67][a,b]	52 [42–68][a,b]	$p < 0.0001$
Minimum diastolic flow velocity, MDV (cm/s)	40 [31–48]	31 [22–37][a]	39 [26–49]	40 [32–53][b]	29 [22–37][a,d]	$p = 0.006$
Mean flow velocity, MFV (cm/s)	57 [49–69]	49 [40–53][a]	46 1[32–56][a]	45 [35–60][a]	42 [33–55][a]	$p = 0.0007$
Pulsatility Index, PI	0.82 [0.69–0.98]	0.94 [0.83–1.18]	0.33 [0.25–0.54][a,b]	0.21 [0.09–0.30][a,b]	0.56 [0.42– 0.75][a,b,d]	$p < 0.0001$
CENTRAL RETINAL ARTERY (CRA)	(*n* = 32)	(*n* = 42)	(*n* = 25)	(*n* = 33)	(*n* = 33)	
Peak systolic flow velocity, PSV (cm/s)	12.3 [9.6–13.1]	9.9 [7.8–12.0]	6.4 [5.0–10.9][a,b]	6.8 [4.9–9.0][a,b]	6.8 [5.2–9.3][a,b]	$p < 0.0001$
Minimum diastolic flow velocity, MDV (cm/s)	3.0 [2.6–3.5]	2.7 [2.0–3.3]	3.9 [2.8–6.4][b]	2.6 [3.5–6.7][a,b,c]	2.6 [1.7–3.6][d]	$p < 0.0001$
Mean flow velocity, MFV (cm/s)	6.6 [5.4–7.4]	5.4 [4.0–6.8]	5 [3.8–8.4]	5.9 [4.4–7.4]	5.4 [4.0–7.0]	$p = 0.13$
Pulsatility Index, PI	1.45 [1.22–1.68]	1.41 [1.18–1.67]	0.56 [0.40–0.83][a,b]	0.33 [0.17–0.45][a,b]	0.8 [0.62–1.03][a,b,d]	$p < 0.0001$

[a] $p < 0.05$ compared with healthy controls.

[b] $p < 0.05$ compared with Heart Failure (HF).

[c] $p < 0.05$ compared with HMII.

[d] $p < 0.05$ compared with HM3 "continuous-flow." Data are shown as median and interquartile range.